Applied Catalysis B: Environmental 113–114 (2012) 126–133

Contents lists available at SciVerse ScienceDirect

Applied Catalysis B: Environmental

journal homepage: www.elsevier.com/locate/apcatb

Use of carbon monoxide and cyanide to probe the active sites on nitrogen-doped carbon catalysts for oxygen reduction

Dieter von Deak, Deepika Singh, Jesaiah C. King, Umit S. Ozkan*

Department of Chemical and Biomolecular Engineering, The Ohio State University, 140 W. 19th Avenue, Columbus, OH 43210, United States

ARTICLE INFO

Article history:
Received 30 June 2011
Received in revised form
14 November 2011
Accepted 17 November 2011
Available online 26 November 2011

Keywords:
CN_x
Nitrogen-doped graphite
Carbon monoxide
Cyanide
Poisoning
Platinum
Oxygen reduction
ORR

ABSTRACT

Interaction of carbon monoxide with CN_x catalysts was investigated using pulse chemisorption, DRIFTS, and cyclic voltammetry techniques. Pulsed chemisorption experiments showed no CO uptake over the CN_x catalysts. Cyclic voltammetry and potential hold studies showed carbon monoxide not to have any electrocatalytic interaction with nitrogen-doped graphite surfaces and not to have any poisoning effect for the oxygen reduction reaction. This is in contrast to the preferential adsorption of CO in the presence of oxygen on ORR sites of Pt catalysts, inhibiting the oxygen reduction activity drastically. Cyanide poisoning experiments performed using KCN showed no activity loss for CN_x, while Pt/VC catalysts showed significant deactivation. These studies suggest that it is unlikely for coordinated metal sites to have significant contribution to the oxygen reduction reaction in CN_x catalysts.

1. Introduction

Hydrogen fuel cells have the potential to transform energy conversion in portable devices if several scientific and economical obstacles could be overcome. Currently, proton exchange membrane (PEM) fuel cell cathodes utilize high loadings of platinum supported on carbon to overcome the slow kinetics of the oxygen reduction reaction (ORR) [1]. Less expensive catalysts consisting of nitrogen-doped graphitic carbon (CN_x) [2–4] or nitrogen-coordinated iron in a carbon matrix (Fe/N/C) have also shown significant oxygen reduction activity under fuel cell conditions and could potentially reduce or replace platinum in PEM fuel cells [5]. However, CN_x catalysts are less active than Pt catalysts, and Fe/N/C catalysts that have high activity deactivate quickly during fuel cell operation [6–9].

The active site ambiguity in CN_x-type electrocatalysts originates from the historical development of these materials. Non-noble metal oxygen reduction catalysts were inspired from hemoglobin where oxygen adsorbs onto an iron center coordinated by four nitrogens (heme site) at low temperatures [10]. Molecules that have a coordinated transition metal, such as iron or cobalt phthalocyanines, are active for ORR in the fuel cell cathode, but quickly deactivate in acidic solution due to metal dissolution causing the destruction of the metal–N_4 oxygen reduction site [11]. In an effort to increase the stability, the metal–N_4 active site materials were placed on a carbon support and subjected to heat treatment in an inert atmosphere, pyrolysis, above 600 °C [12–14]. The pyrolyzed metal–N_4 materials were found to be more stable and surprisingly, more active, but the heat treatment was also found to destroy the coordinated-metal active site, suggesting that a new active site had been formed [15]. More recently, many different ORR catalyst synthesis techniques were reported, utilizing the decomposition of carbon- and nitrogen-containing compounds over a transition metal (Fe, Co) catalyst, and resulting in the growth of nitrogen-doped carbon nanostructures [2–4,16–18]. Some of these synthesis techniques involved a washing process with an acid and/or base to leach out any exposed metal. The residual transition metal remaining in the material was found to be mostly a metal carbide phase encased in carbon [16,19]. Researchers have hypothesized many different active sites for ORR activity in these materials. One proposed site is an active metal center stabilized by nitrogen ligands, similar to those found in macrocycle compounds. These are formed during pyrolysis [5,20–29] and may be located inside the micropores [5,30]. Alternatively, other groups consider non-metallic sites over the graphite structures involving edge nitrogen groups to catalyze oxygen reduction [2–4,16–18,31–41]. One common feature of the two hypothesized types of active sites is that they both would have enhanced ORR

* Corresponding author. Tel.: +1 614 292 6623; fax: +1 614 292 3769.
E-mail address: ozkan.1@osu.edu (U.S. Ozkan).

0926-3373/$ – see front matter © 2011 Elsevier B.V. All rights reserved.
doi:10.1016/j.apcatb.2011.11.029

activity with the inclusion of nitrogen into the hexagonal graphite network [34,40,42–47].

The performance of oxygen reduction electro-catalysts diminishes during long-term operation. This phenomenon is not only present for non-precious metal catalysts, but also occurs for nano-dispersed platinum catalysts. For a carbon-supported platinum oxygen reduction site to be electrochemically active, it must have simultaneous access to protons, oxygen, and electrons at the operating potential [48]. If any one of these conditions is not satisfied, the platinum particle will not participate in oxygen electroreduction. The high potential, strongly acidic and oxidizing environment of the PEM fuel cell cathode causes the electron conducting carbon support to corrode and platinum to separate, decreasing the activity of the catalyst layer [49,50]. Furthermore, platinum has been shown to catalyze the corrosion of the surrounding carbon, leading to the local formation of CO and CO_2 [49,51]. The carbon monoxide that is generated can adsorb more strongly to the platinum catalyst than oxygen, inhibiting oxygen reduction, although the inhibitive effect of CO is much more important over the anode. Fuel cell performance is also diminished by dissolution of platinum in the cathode which either decreases the electroactive area by Ostwald ripening [52] or deposits platinum away from the electrolyte membrane [53].

Similar to platinum, CN_x or Fe/C/N catalysts lose activity during fuel cell operation [8,9]. However, since the active site in these materials is still debated, the mechanism of deactivation is largely unknown. The graphitic nature of carbon materials correlates with corrosion resistance, so unsurprisingly, the stability of CN_x catalysts increases with graphitic character of the material [6,54].

There have been studies in the literature reporting the effect of CO on the oxygen reduction activity of Fe/C/N catalysts. It is known that Fe-porphyrin, a commonly used precursor [6,55,56], has a higher affinity for CO than for oxygen. So, one argument is that, in porphyrins, the hydrophobic pocket created by nitrogen groups around $Fe–N_4$ sites that could improve the O_2 affinity, would also show a similar affinity for CO [57]. However, the studies that explore this effect report different findings. For example, no difference was observed in voltammetric electrochemical capacitance of a carbon-based catalyst, pyrolyzed cobalt porphyrin, when the acid electrolyte was saturated with CO or N_2 [58]. Additionally, no CO adsorption or oxidation peaks were observed in electrochemical capacitance of this catalyst when the electrolyte was saturated with carbon monoxide. However, on a different pyrolyzed metal porphyrin in an acidic electrolyte, a carbon monoxide adduct was detected by X-ray absorption by analyzing the pre-edge features, but this adduct disappeared at >0.6 V vs. NHE [59]. In a recent study, the electrochemical oxygen reduction activity of pyrolyzed Fe-porphyrin catalysts was reported not to be affected by exposure to CO [60]. In other words, when O_2 was replaced with CO at constant voltage, the current dropped quickly to zero, but it increased to its limiting current value immediately upon reintroduction of O_2 into the electrolyte. Although the evidence presented suggests that carbon monoxide has no irreversible effect on $Fe–N_x/C$, it is not clear if there could be competitive and/or preferential adsorption of carbon monoxide in the presence of oxygen.

In this article, we present the effect of CO on CN_x materials and use CO adsorption on Pt as a control experiment. Determining the effect of the competitive adsorption of carbon monoxide in the presence of oxygen would provide further insight into the nature of ORR active sites in CN_x-type materials.

Another poison that is used as a probe in this study is cyanide. A recent article has reported a strong poisoning effect of ORR activity over pyrolyzed and unpyrolyzed iron phthalocyanine catalysts by KCN [61]. The conclusion of the report was that the significant decrease observed in ORR onset potential of these catalysts in the presence of cyanide would suggest that the active sites in these materials are Fe-centered. Similar studies are included in this article examining the effect of KCN over CN_x catalysts, again using Pt/VC as a control experiment.

2. Experimental

2.1. Synthesis of CN_x catalysts through acetonitrile decomposition

The synthesis of nitrogen-doped graphite (CN_x) oxygen reduction electrocatalysts used for this study has been described in greater detail elsewhere [62], so it will be summarized only briefly. CN_x growth media was prepared by the incipient wetness impregnation of 2 wt% Fe iron (II) acetate onto a magnesia support. The growth media was dried overnight in air. It was then placed in a furnace, purged with nitrogen, and then heated at 10 °C/min until 900 °C was reached. At 900 °C, the nitrogen gas was saturated with acetonitrile for 2 h to initiate growth of a nanostructured CN_x catalyst. The resulting material was washed in 1 M HCl at 60 °C to remove magnesia and any exposed iron. Then it was rinsed with DI-water and dried in a convection oven at 110 °C. The resulting dry material was considered carbon-containing nitrogen ORR catalyst (CN_x). Although trace amounts of iron are still present in the resulting CN_x catalyst (mostly encased in carbon), the composition primarily consists of carbon, nitrogen and oxygen.

High performance 20 wt% platinum on Vulcan carbon (BASF), Pt/VC, was used as received.

2.2. Electrochemical testing

All electrochemical testing was performed at room temperature.

2.2.1. Catalyst application and electrochemical setup

The ORR activity and selectivity of catalysts was determined by electrochemical half-cell testing with a rotating disk electrode (RDE). Catalyst inks were prepared using a composition of 1:10:160 (by mass) catalyst mixture: 5% Nafion in aliphatic alcohols: 100% ethanol. Inks were low-energy sonicated for 30 min. Catalyst ink was applied to a 0.1256 cm^2 glassy carbon disk, resulting in a catalyst loading of 427 $\mu g/cm^2$. A model PAR 616 RDE setup was connected to a Princeton Applied Research Bistat for electrochemical testing. An Ag/AgCl (saturated KCl) reference electrode and carbon graphite counter electrode were used for the half-cell system. All reported potentials are referenced vs. the normal hydrogen electrode (NHE). The acidic electrolyte used was 0.5 M H_2SO_4 (aq) in CO poisoning experiments.

2.2.2. Chronoamperometric CO poisoning experiment

Oxygen reduction cathodic linear voltage scans were collected by cyclic voltammetry (CV) on the catalyst-coated glassy carbon disk from 1.2 V to 0.0 V to 1.2 V vs. NHE at 10 mV/s, 1000 rpm in 0.5 M H_2SO_4 (aq). Before electrochemical testing, the 100 mL 0.5 M H_2SO_4 electrolyte was saturated with oxygen by bubbling gaseous oxygen through the electrolyte. Immediately, after the electrode was submerged in the electrolyte a CV was collected to determine the initial activity of the catalyst.

After the initial activity CV, a 0.3 V vs. NHE potential hold was induced on catalyst surface while the RDE continuously spun at 1000 rpm and electrolyte was saturated with different treatment gases. At the beginning of the potential hold, the electrolyte was continuously saturated with oxygen at 30 ccm. After 1.5 min at 0.3 V vs. NHE the gas bubbling through the electrolyte was changed to either a mixture of oxygen and argon (50:50), or a mixture of oxygen and carbon monoxide (50:50). After 26.5 min at 0.3 V vs. NHE the gas bubbling through the system was switched back to oxygen. The electrolyte at 0.3 V vs. NHE was allowed to re-saturate with oxygen and the test was terminated after 65 min. For the potential

hold experiments, it was necessary to normalize the recorded currents by largest oxygen reduction current at the beginning of each data set so that trends could be compared.

After the potential hold had concluded, an oxygen reduction cathodic linear voltage scan was collected by cyclic voltammetry from 1.2 V to 0.0 V to 1.2 V vs. NHE at 10 mV/s while the electrode rotated at 1000 rpm to determine the post-treatment activity of the catalyst.

2.2.3. Voltammetric CO poisoning experiment

The 100 mL 0.5 M H_2SO_4 electrolyte was saturated with oxygen by bubbling gaseous oxygen through the electrolyte. Immediately after the electrode was submerged in the electrolyte, CVs from 1.2 V to 0.0 V to 1.2 V vs. NHE at 10 mV/s were collected on the catalyst-coated glassy carbon disk at 1000 and 0 rpm, to ascertain the initial activity of the catalyst and oxygen functional groups, respectively.

After the first CV concluded, the gas bubbling through the electrolyte was changed to either CO or $CO + O_2$ for 30 min. Thirty minutes was sufficient to saturate the electrolyte as demonstrated by the chronoamperometric experiments as previously described. Then, CVs from 1.2 V to 0.0 V to 1.2 V vs. NHE at 10 mV/s were collected in the presence of the treatment gas on the catalyst-coated glassy carbon disk at 1000 and 0 rpm.

Then, gaseous oxygen was bubbled through the electrolyte at 30 ccm for 30 min. A post treatment CV from 1.2 V to 0.0 V to 1.2 V vs. NHE at 10 mV/s on the catalyst-coated glassy carbon disk at 1000 and 0 rpm was collected in the oxygen saturated electrolyte.

Finally, gaseous argon was bubbled through the electrolyte at 30 ccm for 30 min. A background CV from 1.2 V to 0.0 V to 1.2 V vs. NHE at 10 mV/s on the catalyst-coated glassy carbon disk at 1000 and 0 rpm was collected in the argon saturated electrolyte.

2.2.4. Cyclic voltammetry testing

The 100 mL 0.5 M H_2SO_4 electrolyte was saturated with oxygen by bubbling gaseous O_2 through the solution using a diffuser. Immediately after the electrode was submerged in the solution, a CV from 1.2 V to 0.0 to 1.2 V vs. NHE at 10 mV/s on the catalyst-coated carbon disk at 0 rpm was collected. The electrolyte was then saturated with argon by sparging the electrolyte for 30 min. After the electrolyte was saturated with argon, a CV from 1.2 V to 0.0 to 1.2 V vs. NHE at 10 mV/s on the catalyst-coated carbon disk at 0 rpm was collected. The electrolyte was then saturated with carbon monoxide by sparging the electrolyte for 30 min. After the electrolyte was saturated with carbon monoxide a CV from 1.2 V to 0.0 to 1.2 V vs. NHE at 10 mV/s on the catalyst-coated carbon disk at 0 rpm was collected. This process was repeated for CN_x and 20 wt% Platinum on Vulcan carbon (BASF).

2.2.5. Cyanide poisoning

For CN_x, catalyst ink was prepared as previously described, using a ratio of 1:10:160 (by mass) of catalyst: 5% Nafion in aliphatic alcohols: 100% ethanol. The ink was sonicated for 30 min and was applied onto a glassy carbon electrode to obtain a catalyst loading of 427 $\mu g/cm^2$. For 20 wt% Pt–VC, 5 mg catalyst, 1000 μL ethanol and 50 μL Nafion (5 weight%) was sonicated, and 6 μl of the ink was applied to the glassy carbon electrode to obtain a catalyst loading of 29 $\mu g/cm^2$. The catalyst inks were deposited on PAR 616 RDE setup that was connected to a Princeton Applied Research Bistat for electrochemical testing. A silver–silver chloride reference electrode was used. All CVs were performed with fresh catalyst inks in a pH 6 phosphate buffer solution for the background oxygen reduction experiment, and phosphate buffer with 10 mM KCN for the CN^- poisoning experiments, between 1.2 V to 0 V to 1.2 V vs. RHE (for CN_x) and 1.2 V to 0.2 V to 1.2 V vs. RHE (for Pt, to avoid hydrogen evolution) at 1000 rpm. Extreme care was taken to prepare the cyanide-containing phosphate buffer solution in a vented fumehood with proper personal protective equipment to prevent any physical contact or inhalation of cyanide.

2.3. Carbon monoxide pulsed chemisorption

Carbon monoxide pulsed chemisorption experiments where performed at 35 °C on platinum catalysts supported on Vulcan carbon and CN_x using a chemisorption analyzer Autochem II 2920. 50 mg of 20 wt% Pt–VC was placed in a quartz u-tube reactor and purged with He for 30 min to remove all oxygen from the system. In order to carry out a reduction-pretreatment, a temperature ramp of 10 °C/min to 400 °C was initiated, upon which 5% H_2–He was introduced for 30 min. Thereafter, the reactor was cooled to 35 °C in He, and 9 pulses of pure CO each comprised of 574 μl, were introduced at intervals of 2 min into the reactor. Similar experiments were performed with 50 mg of CN_x, using two different CO concentrations, namely 100% CO and 10% CO in He to ensure that any changes in the signal obtained for each pulse can be observed even if the adsorbed amount was very small.

2.4. DRIFTS

Diffuse reflectance infrared Fourier transform (DRIFT) spectroscopy was performed with a Thermo NICOLET 6700 FTIR spectrometer equipped with a liquid-nitrogen-cooled MCT detector and a KBr beam splitter. The experiments were performed using a Smart collector DRIFT environmental chamber with ZnSe windows. Identical experimental conditions were used for both Pt–VC and CN_x catalysts, except for a 10:1 dilution of CN_x with KBr which is transparent to the IR beam, to allow a better resolved spectra to be obtained. Following a He flush at 30 °C for 30 min, reduction under 5% H_2 in He at 400 °C for 30 min was performed, followed by another pretreatment step for 30 min He at 80 °C to desorb any surface species left behind from the hydrogen treatment. The background spectrum was then collected with 500 scans at 40 °C under He flow before the introduction of pure carbon monoxide for 30 min. The flow was then switched back to He and spectra were collected at 0, 8, 16, 22 and 30 min.

3. Results and discussion

3.1. CO poisoning experiments

3.1.1. Electrochemical testing in the presence of CO

To differentiate the loss of activity due to carbon monoxide adsorption from deactivation during a potential hold under ORR conditions, electrodes were held at 0.3 V vs. NHE in an electrolyte continuously saturated with oxygen. Fig. 1 shows the change in the normalized oxygen reduction current with time for CN_x and Pt/VC catalyst when the potential is held at 0.3 V vs. NHE. An unpyrolyzed iron phthalocyanine supported on Vulcan carbon is also included for stability comparison. As seen in the figure, all three catalysts deactivate at varied rates. The negative normalized current corresponding to oxygen reduction decreases the most during the potential hold experiment for the iron phthalocyanine catalyst, indicating that this catalyst is the least stable of the ones studied. Platinum and CN_x both decrease in current density at a similar rate, but the Pt current density decreases at slightly slower rate.

It should be noted that H_2SO_4 is thought to poison platinum catalysts through sulfate poisoning [63], but since the experimental conditions are identical for all electrochemical tests involving Pt/VC catalysts studied, the deactivation would be equivalent for all, thus making any activity differences attributable only to the chemical treatments used. Furthermore, it was reported that there is no difference in ORR activity for CN_x catalysts in H_2SO_4 and $HClO_4$

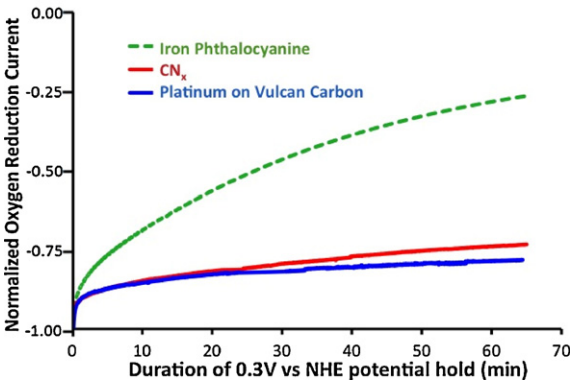

Fig. 1. The change in normalized current density at 0.3 V vs. NHE measured through RDE experiments over CN_x, 20 wt% Pt on Vulcan carbon, 2 wt% Fe (iron phatholocyanine) on Vulcan carbon. (1000 rpm, 0.5 M H_2SO_4 (aq) saturated with oxygen.)

aqueous solutions [64,65], so it is unlikely that sulfate and chloride atoms significantly interact with the CN_x active site.

Carbon monoxide is a known poison for oxygen reduction over platinum electrocatalysts [66,67], so electrochemical activity differences in the presence of CO can be ascribed to carbon monoxide poisoning. Hence, CO poisoning experiments were conducted over Pt/VC and CN_x catalysts under identical conditions for comparison.

Fig. 2 shows four different RDE experiments (performed at a constant potential of 0.3 V vs. NHE), where the gas bubbling (and diffusing) through the electrolyte was changed from O_2 to a mixture or Ar and O_2 (Fig. 2a), or to a mixture of CO and O_2 (Fig. 2b). After 26.5 min, the gas was switched back to O_2. The results are presented as normalized currents where a value of −1 represents the highest reduction current in oxygen at the beginning of the potential hold before the gas was switched. Similar experiments were performed on a platinum catalyst to highlight the difference between CO poisoning and oxygen displacement. Fig. 2a shows the switch from oxygen bubbling through the electrolyte to a 50:50 mixture of O_2 and Ar. The current drops to one half of its original value for both Pt and CN_x catalysts, showing a dilution effect. Fig. 2b shows the switch from O_2 to a 50:50 mixture of O_2 and CO. In this case, the behavior of the CN_x catalyst is identical to that observed when the switch was made to a mixture of Ar and O_2, i.e., only a 50% decrease in current due to dilution, indicating that there is no poisoning or competitive adsorption of CO over this catalyst. For the Pt catalyst however, the current immediately drops to zero, indicating that ORR activity is lost entirely in the presence of CO, due to strong (and preferential) adsorption of CO on the Pt sites. The recovery of the current takes a long time over the Pt catalyst after the gas is switched back to oxygen. A similar catalyst poisoning effect was observed for a 2% CO/H_2 saturated electrolyte when investigating the hydrogen oxidation reaction over high surface area platinum [67].

It should be noted that after the 26.5-min hold period in any gas when the bubbling gas is switched back to O_2, the normalized current does not recover fully, i.e., it does not reach the starting value of −1. This behavior was observed for both CN_x and Pt catalysts. This result is to be expected since a similar deactivation over the same potential hold time was recorded in media saturated with only oxygen saturated, as shown in Fig. 1. The main difference between the two catalysts following CO exposure is in the time it takes for the current to recover. It is an almost immediate recovery over CN_x (within the time it takes for CO to be replaced by O_2 in the

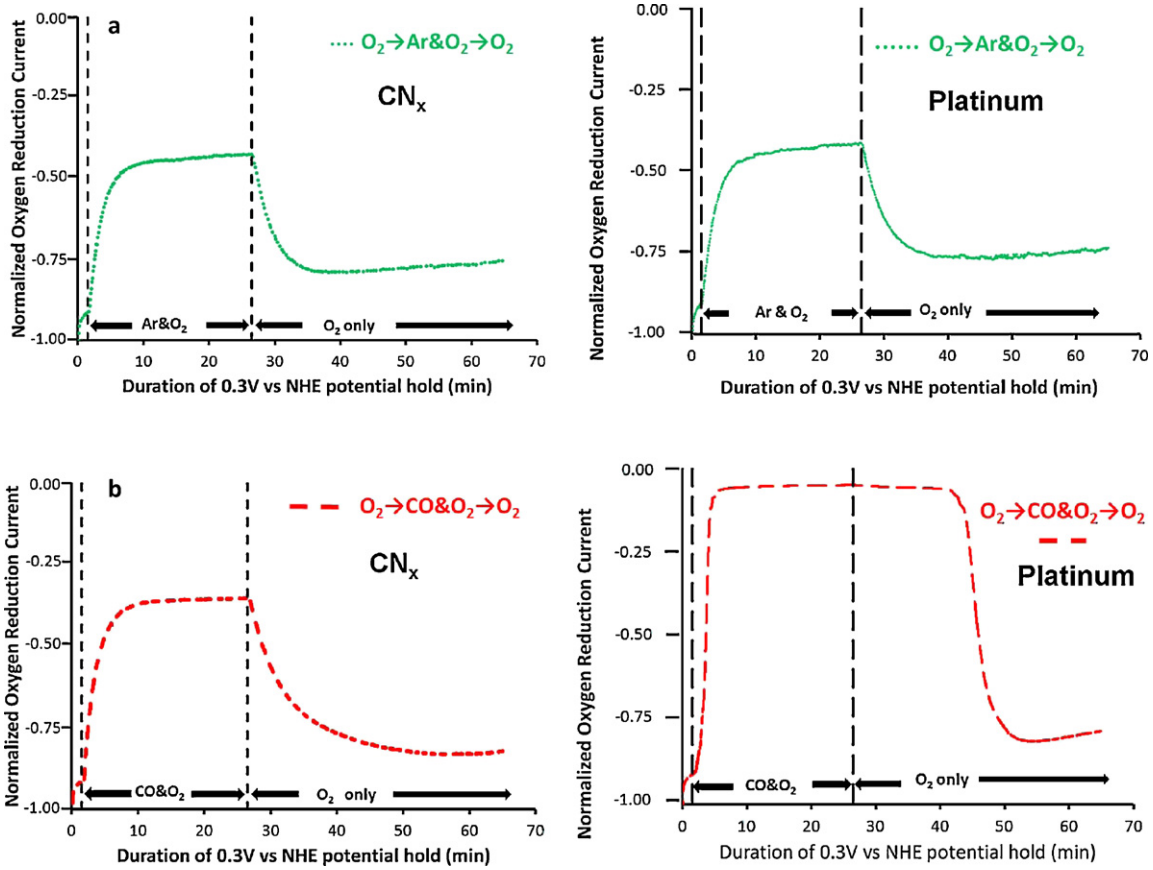

Fig. 2. The change in the normalized current over CN_x (left) and platinum on Vulcan carbon (right) as the oxygen gas bubbling through the electrolyte is replaced by (a) argon and oxygen (b) carbon monoxide and oxygen. (RDE at 0.3 V vs. NHE, 1000 rpm, 0.5 M H_2SO_4 (aq).)

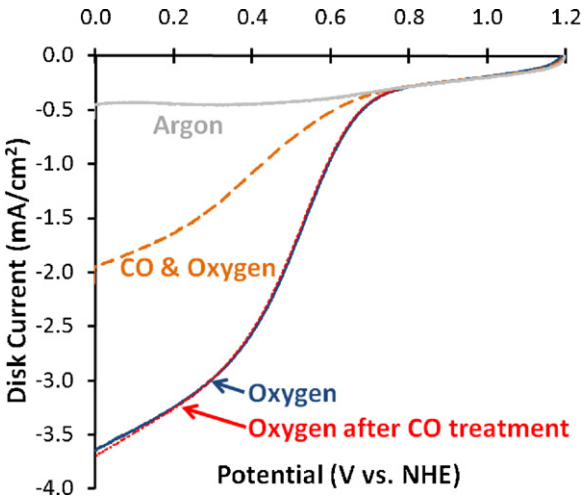

Fig. 3. RDE cathodic potential scans over CN_x catalysts at 5 mV/s from 1.2 V to 0.0 V vs. NHE in 0.5 M H_2SO_4 electrolyte saturated with oxygen, carbon monoxide and oxygen, oxygen after CO treatment, and argon (1000 rpm).

electrolyte) and much slower over Pt (indicating the slow desorption of CO from the ORR sites).

These experiments suggest that the CN_x oxygen reduction active sites do not appreciably bond to carbon monoxide. CO tolerance of these catalysts was also evident in an earlier study where CN_x materials preferentially reduced oxygen in the presence of methanol whereas platinum catalysts were poisoned by carbon monoxide formed as an intermediate from the methanol oxidation reaction [62].

The RDE cathodic potential scans were taken over CN_x catalysts in electrolytes saturated with different gases or gas mixtures, namely, oxygen, carbon monoxide and oxygen, oxygen after CO treatment, and Ar, shown in Fig. 3. As expected, when the

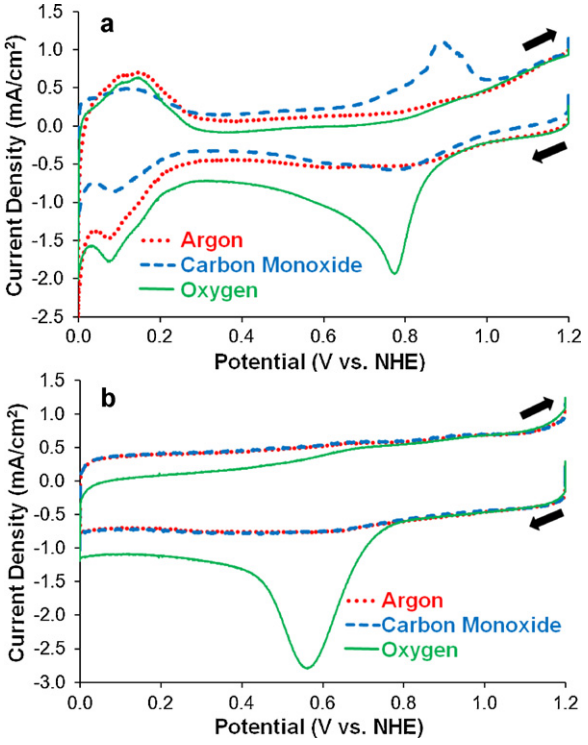

Fig. 4. RDE cyclic voltammograms in 0.5 M H_2SO_4 saturated with argon, carbon monoxide, and oxygen (0 rpm). (a) 20 wt% platinum on Vulcan carbon, (b) CN_x.

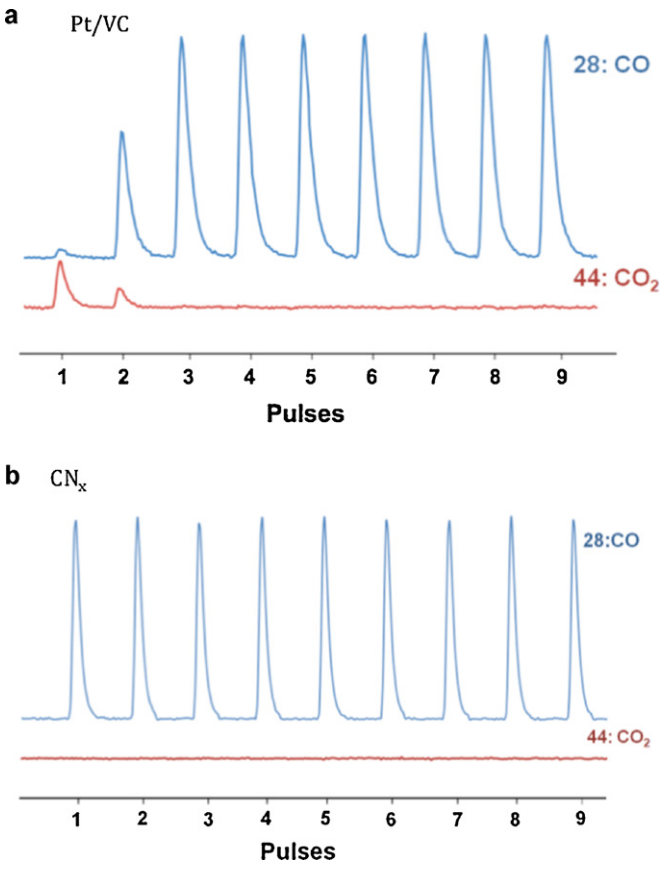

Fig. 5. Carbon monoxide pulse chemisorption on (a) Pt/VC and (b) CN_x catalysts at 35 °C (CO: $m/z = 28$, CO_2: $m/z = 44$).

electrolyte is saturated with both CO and O_2 (50:50), the current density drops by about one half of that observed in pure oxygen. When the scan is repeated in pure oxygen following CO treatment, there is no difference in the disk currents obtained in pure oxygen before or after CO treatment, which supports the results presented in Fig. 2.

To gain additional insight into whether CO adsorbed or interacted with the CN_x catalyst, cyclic voltammograms in electrolytes saturated with argon, carbon monoxide, and oxygen were studied. Similar experiments were conducted with Pt/VC catalyst for comparison (Fig. 4). The catalyst-coated electrodes were not subjected to any additional treatments. Over the Pt/VC catalyst, carbon monoxide is seen to oxidize, as evidenced by the peak at 0.9 V vs. NHE on the anodic scan in CO-saturated electrolyte (Fig. 4a) [68]. Furthermore, the decrease in the current density over the Pt/VC catalyst in the potential range of 0.2 to 0.0 V vs. NHE in CO compared to argon-saturated electrolyte corresponds to a decrease in the H^+ adsorption and desorption, showing a clear poisoning effect. This suggests that proton adsorption is restricted by carbon monoxide adsorbed on the platinum sites. The CVs obtained over the CN_x catalyst, however, are identical regardless of whether the electrolyte is saturated with argon or CO, clearly showing that there is no electrochemical interaction of CO with any site over this catalyst (Fig. 4b).

3.1.2. Pulsed chemisorption

Although neither a poisoning effect of CO nor any electrochemical interaction with the CN_x sites was observed, the electrochemical experiments described above could not definitively determine if there was CO adsorption on CN_x surfaces. To answer this question, pulsed chemisorption at 35 °C experiments were performed using

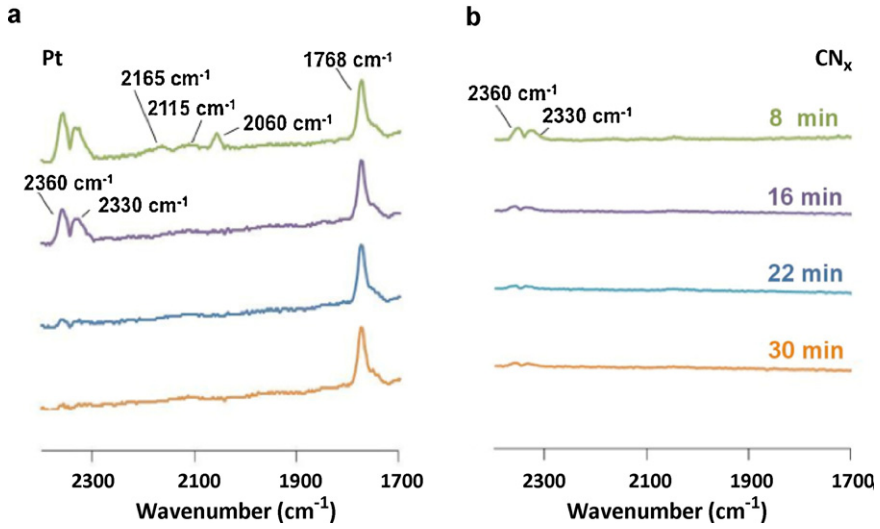

Fig. 6. DRIFT spectra obtained over (a) 20 wt% Pt–VC and (b) CN_x catalysts under He for 8, 16, 22 and 30 min after CO treatment for 30 min at 40 °C.

carbon monoxide as the adsorbate. A series of nine 574 μl pulses of pure carbon monoxide were introduced to the catalyst bed and CO uptake was monitored through the change in the peak area that corresponded to CO not adsorbed by the catalyst in each pulse. Similar experiments were also performed over the Pt/VC catalyst for comparison. Pt/VC catalyst was seen to adsorb CO in the first two pulses (Fig. 5a). There was also CO_2 formation observed as a result of interaction of CO with the Pt sites. CO_2 formation suggests a possible contribution from Boudouard reaction. Although the temperature is quite low, the thermodynamics is certainly favorable for this reaction in the low temperature range used for these experiments.

Over the CN_x catalyst, there was no CO uptake (Fig. 5b). The experiment was repeated over the CN_x catalyst with a more dilute CO stream (10% CO in He) to see if there were small changes in the pulse areas, but the results were the same. These experiments confirmed that CO is adsorbed to platinum supported on Vulcan carbon and not adsorbed on CN_x catalysts. This result supported the earlier assertions that any iron species left in these materials from the leaching process was either encased in carbon sheets and mostly in a carbide phase, and not catalytically accessible [16] or totally inert to any interaction with CO.

3.1.3. DRIFTS

The interaction of CO with the catalyst surfaces was also examined through DRIFT spectroscopy. As shown in Fig. 6a, following CO adsorption, when the gas stream is switched to He, bands at 2165 cm^{-1}, 2115 cm^{-1}, 2060 cm^{-1} and 1768 cm^{-1} are observed over the Pt/VC catalyst. The first two bands are associated with gas phase CO. The 2060 cm^{-1} band can be attributed to linearly adsorbed CO on Pt [69,70]. The band at 1768 cm^{-1} can be due to a bridge or multi-bonded CO species [71], although it is at a lower frequency than what is reported for CO bridging two Pt sites. There have also been reports of Pt carbonyls exhibiting bands in this frequency range [72,73]. This band maintains its intensity even after 30 min of flushing with He after the CO flow is stopped, but the band attributed to linearly adsorbed CO disappears after ~15 min. If linearly adsorbed CO species are responsible for blocking the ORR sites, this result is consistent with what is observed in the RDE studies, which showed complete loss of activity for ORR when CO was mixed with O_2, but gradual recovery of activity several minutes after CO was switched off (Fig. 2). There are also bands indicating formation CO_2 on the surface (2330 and 2360 cm^{-1}), which is consistent with what is observed in CO pulse experiments (Fig. 5a). When a similar experiment was performed over CN_x, the bands due to gas phase CO were barely visible after the gas stream was switched to He (Fig. 6b). There were also weak bands due to CO_2, but no other bands, which would signal a strong interaction of CO with the CN_x surfaces, were observed.

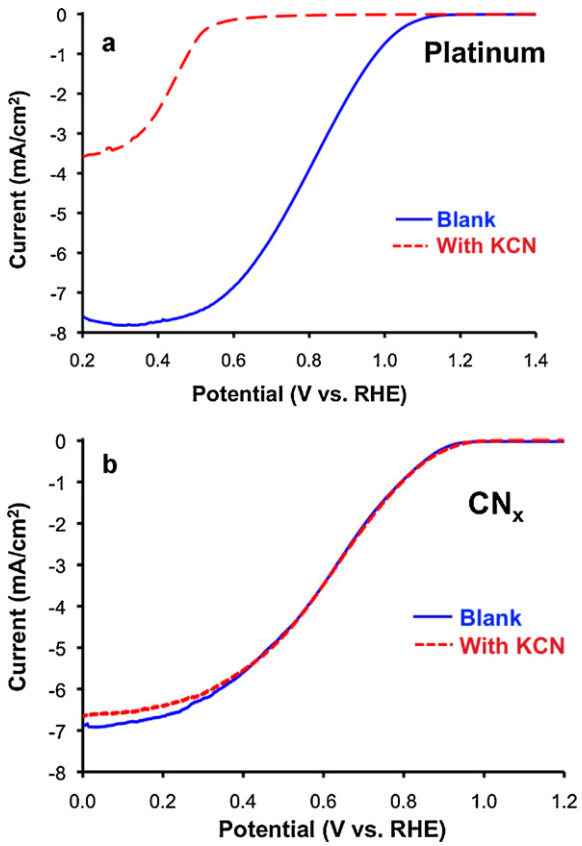

Fig. 7. RDE cathodic polarization curves of (a) 20 wt% Pt–VC, (b) CN_x, in phosphate buffer solution (blue-solid line) and phosphate buffer + 10 mM KCN (red-broken line). Scans were performed at 1000 rpm in oxygen saturated solution. (For interpretation of the references to color in this figure legend, the reader is referred to the web version of the article.)

3.2. Cyanide poisoning experiments

To probe the active sites, additional poisoning experiments were conducted using cyanide (KCN) as a poison. The motivation for these studies was a recent article by Thorum et al. [61], who reported pyrolyzed and unpyrolyzed iron phthalocyanine catalysts to show significant poisoning by cyanide. The conclusion of the report was that the significant decrease observed in ORR onset potential of these catalysts in the presence of cyanide would suggest that the active sites in these materials are Fe-centered.

Fig. 7a and b shows the RDE measurements performed over Pt/VC and CN_x, respectively, to examine the effect of cyanide in their ORR activity. These experiments were modeled after an ORR catalyst poisoning study performed by Gewirth and co-workers [61], but an acidic medium was chosen in our study to make the conditions more relevant for ORR in the PEM fuel cell environment. It should be noted that although the pHs used in our study and in the one by Gewirth's group [61] are different, the authors of that study concluded that the inhibition they observed was "due to cyanide binding and not an artifact arising from the change in electrolyte pH". Scans taken in the absence and presence of cyanide are presented in the same figures. The Pt/VC catalyst shows a clear poisoning effect, with a decrease in onset potential over 450 mV. The significant decrease in limiting current suggests a loss of Pt sites, possibly due to leaching. This may not be surprising since leaching of supported Pt and Au by cyanide has been reported previously [74,75]. Interestingly, there is no poisoning effect observed for the CN_x catalysts in the presence of cyanide. The onset potential and the current density are identical in the scans run with and without KCN (Fig. 7b). This result suggests that in the CN_x materials prepared by acetonitrile decomposition over a metal-doped oxide support may not have metal-centered ORR active sites.

4. Conclusions

Interaction of carbon monoxide with CN_x catalysts was investigated through pulsed chemisorption, DRIFTS and electrochemistry techniques. A commercial Pt catalyst supported on VC was used for comparison and to verify the validity of the techniques used for observing CO poisoning effects. Carbon monoxide was seen not to adsorb on CN_x surfaces, as shown by pulsed chemisorption experiments. The DRIFTS experiments also showed no major interaction with the surface. Rotating disk electrode experiments performed showed that there was no inhibitive effect of CO on ORR activity when both CO and O_2 were present in the electrochemical medium. Cyclic voltammetry tests conducted in electrolytes saturated with CO showed no electrocatalytic interaction of CO with CN_x surfaces. These results were in clear contrast to what was observed over the Pt/VC catalysts, which showed a preferential adsorption of CO to ORR sites in the presence of O_2, causing total loss of activity. The blockage of ORR sites was reversible once CO was removed from the system. These studies showed that ORR activity of CN_x catalysts were not affected by the presence of CO. These results may not be sufficient to draw any conclusions about the absence or presence of a metal-centered active site, but they suggest that if there are metal sites present on these materials, they are either not accessible or completely inert for any interaction with CO.

Cyanide poisoning was used to probe the active sites, since cyanide is known to strongly interact with most metals and it was shown to poison Fe/C/N catalysts [61]. Although Pt/VC catalyst, which was used as a control experiment, showed very significant decrease in onset potential, for CN_x catalysts, the onset potential and the current density remained unchanged in the scans run with and without KCN. This result suggests that the active sites in CN_x catalysts do not involve metal centers.

It appears that the two classes of catalysts, often denoted in the literature as Fe/C/N and CN_x are quite different materials. Fe/C/N catalysts often prepared by supporting a macrocycle on a carbon support do have a metal center. Some of these materials go through pyrolysis in an inert or nitrogen-containing environment, but there is never a washing step in their preparation to leach out the metal. It is expected that a metal center that was part of the starting macrocycle still remains in these materials, although its exact nature may not yet be fully elucidated.

The CN_x catalysts reported in our studies, on the other hand, are prepared by pyrolyzing a carbon–nitrogen source, such as acetonitrile, over a growth medium. Most often, the support is an oxide (alumina, silica, magnesia), either used alone [2] or doped with a transition metal (Fe or Co). Through acetonitrile pyrolysis, significant carbon growth has been documented on these media in our earlier studies [3,4,17,18]. These materials then go through a washing step with a strong acid or a base. Following this step, the resulting materials are graphitic carbon with different nanogeometries and high nitrogen content [32,76]. Any transition metal left behind cannot be detected by surface analysis techniques, such as XPS. The iron species left behind in catalysts grown on Fe-doped oxide supports were characterized by TEM, Mössbauer, and XAFS studies [16,19,32], which showed Fe to be primarily encased in carbon, exhibiting mostly a cementite-type carbide phase. These species do not interact with CO, H_2S [19], or cyanide.

There remain many questions about the nature of active sites in Fe/N/C and CN_x catalysts, but it appears that the ORR activity in these materials could stem from different active sites. Presence of more than one type of active site on each class of materials cannot be ruled out either.

Acknowledgement

This work was supported by the U.S. Department of Energy, Office of Science, Office of Basic Energy Sciences, under contract no. DE-FG02-07ER15896.

References

[1] H.A. Gasteiger, N.M. Markovic, Science 324 (2009) 48–49.
[2] P.H. Matter, U.S. Ozkan, Catal. Lett. 109 (2006) 115–123.
[3] P.H. Matter, E. Wang, M. Arias, E.J. Biddinger, U.S. Ozkan, J. Mol. Catal. 264 (2007) 73–81.
[4] P.H. Matter, E. Wang, M. Arias, E.J. Biddinger, U.S. Ozkan, J. Phys. Chem. B 110 (2006) 18374–18384.
[5] M. Lefevre, E. Proietti, F. Jaouen, J.-P. Dodelet, Science 324 (2009) 71–74.
[6] H. Meng, N. Larouche, M. Lefevre, F. Jaouen, B. Stansfield, J.P. Dodelet, Electrochim. Acta 55 (2010) 6450–6461.
[7] X. Li, G. Liu, B.N. Popov, J. Power Sources 195 (2010) 6373–6378.
[8] F. Jaouen, E. Proietti, M. Lefevre, R. Chenitz, J.P. Dodelet, H.T. Chung, C.M. Johnston, P. Zelenay, Energy Environ. Sci. 4 (2011) 114–130.
[9] R. Borup, J. Meyers, B. Pivovar, Y.S. Kim, R. Mukundan, N. Garland, D. Myers, M. Wilson, F. Garzon, D. Wood, P. Zelenay, K. More, K. Stroh, T. Zawodzinski, J. Boncella, J.E. McGrath, M. Inaba, K. Miyatake, M. Hori, K. Ota, Z. Ogumi, S. Miyata, A. Nishikata, Z. Siroma, Y. Uchimoto, K. Yasuda, K.-I. Kimijima, N. Iwashita, Chem. Rev. 107 (2007) 3904–3951.
[10] B. Alberts, A. Johnson, J. Lewis, M. Raff, K. Roberts, P. Walter, Molecular Biology of the Cell, 4th ed., Garland science, New York, 2002.
[11] H. Jahnke, M. Schonborn, G. Zimmerman, Fortschr. Chem. Forsch. 61 (1976) 133.
[12] K. Wiesener, Electrochim. Acta 31 (1986) 1073–1078.
[13] E. Yeager, Electrochim. Acta 29 (1984) 1527–1537.
[14] J.A.R. van Veen, J.F. van Baar, K.J. Kroese, Chem. Soc. Faraday Trans. I 77 (1981) 2827.
[15] P. Gouerec, M. Savy, Electrochim. Acta 44 (1999) 2653–2661.
[16] P.H. Matter, E. Wang, J.-M.M. Millet, U.S. Ozkan, J. Phys. Chem. C 111 (2007) 1444–1450.
[17] P.H. Matter, E. Wang, U.S. Ozkan, J. Catal. 243 (2006) 395–403.
[18] P.H. Matter, L. Zhang, U.S. Ozkan, J. Catal. 239 (2006) 83–96.
[19] D. von Deak, D. Singh, E.J. Biddinger, J.C. King, B. Bayram, J.T. Miller, U.S. Ozkan, J. Catal., in press, doi:10.1016/j.jcat.2011.09.027.
[20] J. Herranz, F. Jaouen, J.-P. Dodelet, ECS Trans. 25 (2009) 117–128.
[21] T. Schilling, M. Bron, Electrochim. Acta 53 (2008) 5379–5385.

[22] M. Bron, P. Bogdanoff, S. Fiechter, H. Tributsch, J. Electroanal. Chem. 578 (2005) 339–344.
[23] J. Maruyama, I. Abe, J. Electrochem. Soc. 154 (2007) B297–B304.
[24] V.S. Tyurin, K.A. Radyushkina, O.A. Levina, M.R. Tarasevich, Russ. J. Electrochem. 37 (2001) 843–847.
[25] A.L. Bouwkamp-Wijnoltz, W. Visscher, J.A.R. van Veen, E. Boellaard, A.M. van der Kraan, S.C. Tang, J. Phys. Chem. B 106 (2002) 12993.
[26] A.B. Anderson, R.A. Sidik, J. Phys. Chem. B 108 (2004) 5031–5035.
[27] M. Jian, S.-H. Chou, A. Siedle, J. Phys. Chem. B 110 (2006) 4179–4185.
[28] G.C.-K. Liu, J.R. Dahn, Appl. Catal. A: Gen. 347 (2008) 43–49.
[29] T.S. Olson, S. Pylypenko, J. Fulghum, P. Atanassov, J. Electrochem. Soc. 157 (2010) B54–B63.
[30] M. Lefevre, J.-P. Dodelet, Electrochim. Acta 53 (2008) 8269–8276.
[31] J.-I. Ozaki, K. Nozawa, K. Yamada, Y. Uchiyama, Y. Yoshimoto, A. Furuichi, T. Yokoyama, A. Oya, L.J. Brown, J.D. Cashion, J. Appl. Electrochem. 36 (2006) 239–247.
[32] E.J. Biddinger, U.S. Ozkan, J. Phys. Chem. C 114 (2010) 15306–15314.
[33] S. Maldonado, K.J. Stevenson, J. Phys. Chem. B 109 (2005) 4707–4716.
[34] S.M. Lyth, Y. Nabae, S. Moriya, S. Kuroki, M.-A. Kakimoto, J.-I. Ozaki, S. Miyata, J. Phys. Chem. C 113 (2009) 20148–20151.
[35] Y. Nabae, S. Moriya, K. Matsubayashi, S.M. Lyth, M. Malon, L. Wu, N.M. Islam, Y. Koshigoe, S. Kuroki, M. Kakimoto, S. Miyata, J. Ozaki, Carbon 48 (2010) 2613–2624.
[36] V.Z. Barsukov, V.G. Khomenko, A.S. Katashinskii, T.I. Motronyuk, Russ. J. Electrochem. 40 (2004) 1170–1173.
[37] S.A. Kumar, S.-M. Chen, Biosens. Bioelectron. 22 (2007) 3042–3050.
[38] S.A. Kumar, S.-M. Chen, J. Mol. Catal. A: Chem. 278 (2007) 244–250.
[39] P. Gouerec, A. Biloul, O. Contamin, G. Scarbeck, M. Savy, J. Riga, L.T. Weng, P. Bertrand, J. Electroanal. Chem. 422 (1997) 61.
[40] N.P. Subramanian, X. Li, V. Nallathambi, S.P. Kumaraguru, H. Colon-Mercado, G. Wu, J.-W. Lee, B.N. Popov, J. Power Sources 188 (2009) 38–44.
[41] J.-I. Ozaki, S.-I. Tanifuji, A. Furuichi, K. Yabutsuka, Electrochim. Acta 55 (2010) 1864–1871.
[42] K. Prehn, A. Warburg, T. Schilling, M. Bron, K. Schulte, Compos. Sci. Technol. 69 (2009) 1570–1579.
[43] F. Jaouen, M. Lefevre, J.-P. Dodelet, M. Cai, J. Phys. Chem. B 110 (2006) 5553–5558.
[44] F. Jaouen, S. Marcotte, J.-P. Dodelet, G. Lindbergh, J. Phys. Chem. B 107 (2003) 1376–1386.
[45] Z. Ma, J. Shi, Y. Song, Q. Guo, G. Zhai, L. Liu, Carbon 44 (2006) 1298–1352.
[46] J.-I. Ozaki, T. Anahara, N. Kimura, A. Oya, Carbon 44 (2006) 3358–3361.
[47] J.-I. Ozaki, N. Kimura, T. Anahara, A. Oya, Carbon 45 (2007) 1847–1853.
[48] W. Vielstich, H.A. Gasteiger, A. Lamm (Eds.), Handbook of Fuel Cells—Fundamentals, Technology and Applications, John Wiley & Sons, Ltd., 2003.
[49] L.M. Roen, C.H. Paik, T.D. Jarvi, Electrochem. Solid-State Lett. 7 (2004) A19–A22.
[50] A.P. Young, J. Stumper, E. Gyenge, J. Electrochem. Soc. 156 (2009) B913–B922.
[51] A.M. Chaparro, N. Mueller, C. Atienza, L. Daza, J. Electroanal. Chem. 591 (2006) 67–73.
[52] Z.Y. Liu, J.L. Zhang, P.T. Yu, J.X. Zhang, R. Makharia, K.L. More, E.A. Stach, J. Electrochem. Soc. 157 (2010) B906–B913.
[53] J. Xie, D.L. Wood III, D.M. Wayne, T.A. Zawodzinski, P. Atanassov, R.L. Borup, J. Electrochem. Soc. 152 (2005) A104–A113.
[54] K. Kinoshita, Carbon, Electrochemical and Physiochemical Properties, Wiley Interscience, New York, 1988.
[55] A.A. Serov, M. Min, G. Chai, S. Han, S.J. Seo, Y. Park, H. Kim, C. Kwak, J. Appl. Electrochem. 39 (2009) 1509–1516.
[56] X. Li, C. Liu, W. Xing, T. Lu, J. Power Sources 193 (2009) 470–476.
[57] C. Ruzie, P. Even, D. Ricard, T. Roisnel, B. Boitrel, Inorg. Chem. 45 (2006) 1338–1348.
[58] T.S. Olson, B. Blizanac, B. Piela, J.R. Davey, P. Zelenay, P. Atanassov, Fuel Cells 5 (2009) 547–553.
[59] I.T. Bae, D. Scherson, J. Phys. Chem. B 102 (1998) 2519–2522.
[60] L. Birry, J.H. Zagal, J.P. Dodelet, Electrochem. Commun. 12 (2010) 628–631.
[61] M.S. Thorum, J.M. Hankett, A.A. Gewirth, J. Phys. Chem. Lett. 2 (2011) 295–298.
[62] E.J. Biddinger, U.S. Ozkan, Top. Catal. 46 (2007) 339–348.
[63] K.-L. Hsueh, E.R. Gonzalez, S. Srinivasan, Electrochim. Acta 28 (1983) 691–697.
[64] S. Gojkovic, S. Gupta, R. Savinell, J. Electroanal. Chem. 462 (1999) 63–72.
[65] F. Jaouen, J. Herranz, M. Lefevre, J.-P. Dodelet, U.I. Kramm, I. Herrmann, P. Bogdanoff, J. Maruyama, T. Nagaoka, A. Garsuch, J.R. Dahn, T.S. Olson, S. Pylypenko, P. Atanassov, E.A. Ustinov, ACS Appl. Mater. Interfaces 1 (2009) 1623–1639.
[66] I.T. Bae, D. Scherson, J. Phys. Chem. 100 (1996) 19215–19217.
[67] T.J. Schmidt, H.A. Gasteiger, R.J. Behm, J. Electrochem. Soc. 146 (1999) 1296–1304.
[68] A. Pozio, M.D. Francesco, A. Cemmi, F. Cardellini, L. Giorgi, J. Power Sources 105 (2002) 13–19.
[69] J. Rasko, J. Catal. 217 (2003) 478–486.
[70] R.M. Rioux, J.D. Hoefelmeyer, M. Grass, H. Song, K. Niesz, P. Yang, G.A. Somorjai, Langmuir 24 (2008) 198–207.
[71] H. Gao, X. Wenqing, H. Hong, S. Xiaoyan, X. Zhang, K.-I. Tanaka, Spectrochim. Acta Part A: Mol. Biomol. Spectrosc. 71 (2008) 1193–1198.
[72] A.I. Serykh, O.P. Tkachenko, V.Y. Borovkov, V.B. Kazansky, M. Beneke, N.I. Jaeger, G. Schulz-Ekloff, Phys. Chem. Chem. Phys. 2 (2000) 5647–5652.
[73] A.A. Taimoor, I. Pitault, F.C. Meunier, J. Catal. 278 (2011) 153–161.
[74] Q. Fu, H. Saltsburg, M. Flytzani-Stephanopoulos, Science 301 (2003) 935–938.
[75] W. Deng, J. De Jesus, H. Saltsburg, M. Flytzani-Stephanopoulos, Appl. Catal. A: Gen. 291 (2005) 126–135.
[76] E.J. Biddinger, D.S. Knapke, D. von Deak, U.S. Ozkan, Appl. Catal. B: Environ. 96 (2010) 72–82.